OPTIMIZATION OF OXIDANT AGENT IN THE PHOTOCATALYTIC DEGRADATION OF ETHIDIUM BROMIDE WITH TiO_2 AND IRON-DOPED TiO_2 CATALYSTS

J. Carbajo, C. Adán, A. Rey, A. Martínez-Arias, A. Bahamonde
Instituto de Catálisis y Petroleoquímica, CSIC, C/ Marie Curie Nº. 2, 28049 Madrid (Spain).

Abstract

A series of nanosized iron-doped titania catalysts have been studied for photocatalytic degradation of Ethidium Bromide (EtBr) with oxygen. The reaction mechanism of EtBr photocatalytic degradation can be strongly affected by the degree of EtBr surface adsorption most favored over basic titania surfaces such as those present in undoped TiO_2 and Fe-TiO_2 with low iron content. On the contrary, EtBr removal took fundamentally place by heterogeneous photocatalysis in doped titania catalysts with iron content higher than 0.7 wt%. The efficiency in the use of H_2O_2 has been studied in order to define optimum operating conditions under which total EtBr conversion and significant TOC removal were achieved. The study has demonstrated that H_2O_2 dosing during the course of the reaction could minimize H_2O_2 scavenging effects and improve overall degree of EtBr mineralization. The stability and durability of a selected iron-doped TiO_2 catalyst has been examined by performing five consecutive cycles of nine hours each and using punctual H_2O_2 dosing. Such catalyst is able to perform at constant activity level during at least four consecutive runs achieving total EtBr conversion and 80% of mineralization.

Keywords: Photocatalysis, Ethidium Bromide, nanostructured iron-doped TiO_2, H_2O_2 dosage.

I. Introduction

Ethidium bromide (EtBr) is commonly used as a non-radioactive marker for identifying and visualizing nucleic acid bands in electrophoresis and in other methods of gel-based nucleic acid separation [1]. EtBr is a dark red, crystalline, non-volatile solid, moderately soluble in water, which fluoresces readily with a reddish-brown color when exposed to ultraviolet light (UV). Its formula, 2,7,-diamino-10-ethyl-9-phenyl-phenanthridium bromide, $C_{21}H_{20}N_3 \cdot Br$, and molecular structure are shown in Scheme 1.a.

It is known that EtBr constitutes one of the most important and useful tools for the study of secondary and tertiary structures of DNA as a consequence of its high specific ability towards reaction with nucleic acids [2]. However, this property has made EtBr to be one of the most mutagenic compounds due to the fact that when EtBr is intercalated between the bases pairs of DNA, it promotes the local untwisting of the double-helix (see Scheme 1.b). Therefore, although it is an effective tool, its hazardous properties (it is moderately toxic and strongly mutagenic and teratogenic) require special safe handling and disposal procedures [3].

Nowadays, different methods have been employed for removing EtBr from aqueous solutions. These include biomaterials filters based in DNA films, which can be activated by means of UV light irradiation, macro-reticular resins used to capture traces [4], porous particles of poly(ether sulphone) loaded with DNA as well as columns able to accumulate harmful DNA-intercalant contaminants from diluted aqueous solution of EtBr [5,6,7]. Nevertheless, total EtBr chemical degradation is complicate and requires the employment of expensive reactants which increases the price of wastewater treatment [8]. In turn, it must be considered that the toxicity of by-products generated during its chemical or biological degradation could be higher than original EtBr itself.

Additionally, in most cases the decontamination methods used to capture EtBr waste are related to a final incineration process. As an example, Massachusetts Institute of Technology generated approximately 4.7 tons of EtBr wastes in 2005. Among possible treatments, incineration was chosen to achieve total EtBr degradation [9]. However, incineration is an expensive process (300 $ per 55-gallon drum) [9], mainly as a consequence of required energy input. Additionally,

such high price is also due to the fact that the combustion gases contain halogenated molecules, as elementary bromine or free bromide as well as hydrobromic acid, which pose the need of special treatments in the incinerator system to avoid their discharges into the atmosphere.

Nowadays, advanced oxidation processes (AOPs) such as heterogeneous photocatalysis appear as one of the most attractive methods for the treatment of wastewater with relatively low organic pollutant concentrations [10]. Among these photocatalytic processes, those based on the employment of titania semiconductors excitable by solar light, are appearing as an interesting alternative to conventional processes since most harmful and toxic organic pollutants could be completely mineralized to carbon dioxide and water by means of the strong oxidizing power of photo-generated species in titania [11].

In spite of the large number of examined detoxification methods for EtBr removal, only a few works are focussed on heterogeneous photocatalysis. In this sense Faisal et al. [12] have described the behaviour of three different commercially available TiO_2 powders for the photocatalytic degradation of two dyes, Acridine orange and EtBr. In turn, previous papers from our group have reported the possibility to employ photocatalytic oxidation for total EtBr removal from diluted aqueous solutions using various titanium dioxide samples as photocatalyst and solar light [13,14]. Following such reports, the aim of this work has consisted in analyzing the influence of two oxidant agents, such as oxygen and hydrogen peroxide, on the photocatalytic degradation of diluted solutions of EtBr with iron-doped titania catalysis. From a comparative study with titania catalysts doped with iron at different levels and employing oxygen as oxidant agent, an intermediate iron content (about 0.7 wt. %) was selected for the optimum photocatalyst on the basis of overall photodegradation parameters.

In heterogeneous photocatalytic process employing titania based catalysts it is very common the use of oxygen from the air as oxidant taking into account its good efficiency, availability and low cost. Nevertheless, it is known that other oxidant agents such as hydrogen peroxide can be more efficient to generate hydroxyl radicals with a high capability towards organic matter oxidation [15]. On this basis, the efficiency of hydrogen peroxide for EtBr photooxidation has been

also studied in order to define the best operating conditions under which total EtBr conversions and TOC removal could be reached.

The present work has demonstrated that hydrogen peroxide dosing control along irradiation time can minimize auto-scavenging reactions allowing an important improvement in the level of final organic matter removal. Additionally, the stability and durability of the mentioned selected iron-doped catalyst during EtBr photo-oxidation has been checked during five consecutive reaction cycles with optimized operating conditions and using H_2O_2 as oxidant agent.

2. Experimental

2.1 Catalyst Synthesis

Five home made iron-doped TiO_2 catalysts were prepared using a combined sol-gel/reverse microemulsion method described elsewhere [16,17]. All amorphous mixed oxides (after overnight drying at 100 ^oC) were calcined at 450ºC for 2 hours under air atmosphere. Iron content in the doped titania catalysts varied from 0.5, 1, 2 to 5 wt. %, which produced appreciable differences in the pH values of the water phases within the respective microemulsions [18].

2.2 Characterization Studies

Structural characterization of the powder samples was analyzed by means of X-ray diffraction (XRD) with a Siemens D-500 apparatus, using nickel-filtered Cu Kα radiation operating at 40 kV and 40 mA, with a 0.04° step size and accumulating a total of 5 s per point. Crystal particle sizes were obtained by means of Scherrer equation [19].

The specific surface areas, S_{BET}, were obtained from nitrogen adsorption-desorption isotherms at -196ºC using a Micrometritics Tristar automatic apparatus on samples previously outgassed overnight at 140 ºC to a vacuum of < 10^{-4} Pa to ensure a dry clean surface free from any loosely held adsorbed species.

Catalyst surface characterization was performed by X-ray photoelectron spectroscopy (XPS) with a VG Escalab 200R spectrometer employing an Mg Kα (1253.6eV) X-ray source. The binding energies (BE) were referenced to the spurious C1s peak (284.6 eV) used as an internal standard to take into account

charging effects. The areas of the peaks were computed by fitting the experimental spectra to Gaussian/Lorentzian curves after removal of the background (Shirley function). Surface atomic ratios were calculated from peak area ratios normalized by the appropriate atomic sensitivity factors [20]. Iron content of the catalysts was analyzed by a Perkin Elmer ICP-OES, Model optima 3300 DV after acid digestion, via microwave (see Table 1).

Ammonia adsorption at room temperature, measured on an ASAP-2010C instrument (Micromeritics), was used to evaluate surface acidity, expressed as meq of ammonia adsorbed per gram of sample. The samples were first outgassed at 350 ºC for 2 h, and then cooled to 30 °C before determining the ammonia physisorption plus chemisorption capacity. Subsequently, after outgassing the samples at 30°C for 4 h to remove the physisorbed gas, a second adsorption process was carried out to obtain the final chemisorbed amount by difference between the two isotherms.

Mass tritation of aqueous slurries of the catalysts, was carried out following the method described elsewhere [14]. For this purpose 0.5 g of titania based catalysts was added to 10 mL of CO_2-free distilled water kept in a bottle at room temperature and continuously stirred for 1 day until the pH of the slurry was stabilized.

Some basic physico-chemical properties of the catalysts are summarized in Table 1. From XRD patterns (not shown), anatase titania crystalline phase has been always detected without any apparent evidence of iron-containing phases. All studied catalysts have presented an anatase crystal size around 10 nm; maximum size was found for intermediate iron-doped titania catalysts, which has basically been attributed to maximization of iron incorporation into anatase phase, as detailed elsewhere [18]. Concerning textural properties, minimum surface area values are also observed for intermediate iron loading specimens, suggesting a certain correlation with mean crystal size values.

2.3 Photocatalytic Activity Studies

EtBr adsorption runs were carried out in batch reactors with 50 mL glass bottles at ambient conditions and initial pH of 6.5 (which corresponds to the pH of 20 mg L^{-1} solution of EtBr in distilled water). An amount of 0.01 g of catalyst was used in this adsorption study and adsorption equilibrium was shown to be attained after about one hour.

EtBr photocatalytic activity runs were carried out in a 1 L Pyrex semi-continuous slurry-photoreactor described elsewhere [14], at atmospheric pressure and room temperature. A high-pressure Hg lamp (500 W, Helios Italquartz, Italy) [14], immersed within the suspension and cooled by water circulating through a Pyrex jacket, was used for illumination.

Different operating conditions were employed to analyze the influence of two oxidant agents on EtBr photodegradation. First, a reactant mixture consisting on 20 mg L^{-1} of EtBr at pH 6.5 and 500 mg L^{-1} of catalyst were premixed with 100 Ncm^3 min^{-1} of oxygen flow in dark conditions, during 30 minutes to guarantee homogeneous mixing in the reactor. After that, photocatalytic runs started by turning on the UV lamp. When hydrogen peroxide was used as oxidant, H_2O_2 concentrations of 80 and 160 mg·L^{-1}, corresponding to the theoretical or double of stoichiometric amount to completely oxidize ethidium bromide, respectively, were premixed with 20 mg L^{-1} of EtBr and 500 mg L^{-1} of catalysts. Two initial pH_o values (3.0 and 6.5) were also studied. Again, a first period of 30 minutes under dark conditions was used to guarantee homogeneous mixing in the reactor prior to the photocatalytic run.

To optimize the most appropriate initial H_2O_2 concentration, an oxidant dosing control was carried out. The key factor was introducing the theoretical amount of hydrogen peroxide to completely oxidize the measured TOC in each step, during an overall irradiation time of 9 hours. The initial operating conditions were the following: 20 mg·L^{-1} of EtBr, 500 mg·L^{-1} of TiO_2-Fe1 catalyst, and pH_o=3.

Finally, some photodegradation cycles were carried out with a selected catalyst (TiO_2-Fe1, see Table 1) to analyze catalyst stability and durability in the photocatalytic process under study. The catalyst was recycled after a filtration step and maintaining its concentration in the reaction vessel. Up to five cycles of nine hours each were performed at the following conditions: 20 mg·L^{-1} of EtBr,

500 mg·L^{-1} of TiO_2-Fe1 catalyst, and pH_o=3. Hydrogen peroxide dosages in each irradiation cycle were carried out under the conditions obtained from the dosing control analysis commented above.

In all cases, small portions of the reactant solution were extracted at selected times and EtBr concentration was measured by means of a UV-vis Shimadzu 2100 apparatus for liquid samples upon monitoring the area of the band centered at λ = 480 nm [21].

In addition,,Total Organic Carbon (TOC) was measured with a TOC Analyzer (TOC-$V_{CSH/CSN}$ Shimadzu). Hydrogen peroxide concentrations were determined by colorimetric titration with a UV-Vis Shimadzu spectrometer model 2100 at 410 nm using the titanium sulfate [22].

Iron lixiviates to the reaction media were determined by means of a Perkin Elmer ICP-OES spectrometer at 259.94 nm.

3. Results and discussion

3.1 Ethidium Bromide Adsorption Studies

The influence of iron content along with several physico-chemical properties of the catalysts on EtBr adsorption are summarized in Figure 1. First of all, an important decrease in EtBr adsorption amounts upon increasing the iron content in the catalysts has been observed. Figure 1a compares the surface acidity of the catalysts, based on ammonia adsorption measurements, with EtBr adsorption percentage. It is noticeable the higher adsorption level detected with bare titania catalysts (55 %), for which its weak surface basic character is known to favor EtBr adsorption [14], whereas the catalyst with highest surface acid character (TiO_2-Fe5) presents the lowest EtBr adsorption values. Moreover, it must be noted that according to the results displayed in Figure 1b, the amount of adsorbed EtBr decreases with increasing the surface area of the catalysts. Consequently, surface acid/base character rather than surface area plays the most relevant role in EtBr adsorption. In addition, it can be observed in Figures 1c and 1d that an important decrease in the synthesis pH is produced upon increasing the iron content in the catalysts; this is also in agreement with pH

observed for the aqueous slurries of the catalysts, leading to important changes in their surface acidity.

Therefore, undoped titania and the doped titania catalyst with the lowest iron content display a significant amount of EtBr chemisorption; this must be taken into account during analysis of photocatalytic performance, considering its possible relevancy at a mechanistic level [14,23,24]. In contrast, for iron doping level higher than 0.36 wt. % the surface acquires an acid character which minimizes the capability of the catalyst for EtBr chemisorption.

3.2 Photocatalytic degradation of EtBr with oxygen

Evolutions of EtBr and TOC conversions as a function of reaction time, when oxygen was used as oxidant agent, are shown in Figures 2a and 2b, respectively. The EtBr photolysis, in absence of catalyst, was carried out under the same operating conditions studied here and less than 40% of EtBr conversion with no TOC removal was observed [14].

In general, some differences in total EtBr conversions (Figure 2a) can be observed as a function of the iron content of the catalyst. Whereas total EtBr conversion was detected over undoped titania catalyst at 60 min, higher reaction times were always necessary to get high EtBr conversion levels with iron-doped catalysts. In turn, significant differences can be also observed for TOC conversion (Figure 2b). Whereas undoped titania (TiO_2) and the lowest iron content (TiO_2-Fe0.5) catalysts present maximum TOC conversions at the beginning of the photocatalytic process, a progressive enhancement of TOC removal levels can be observed for the rest of iron-doped titania samples.

It has been already revealed that the reaction mechanism of EtBr photodegradation with bare titania catalysts can be affected by the degree of substrate adsorption on the catalyst surface [14], which, as shown above, is most favored over catalyst surfaces with certain basic character as those of TiO_2 and TiO_2-Fe0.5 catalysts (Fig. 1). This is reflected in the significant EtBr and TOC conversions observed during dark stage for these catalysts. On the contrary, EtBr adsorption can be considered of lower relevancy when iron content was higher than 0.36 wt. %, given that the adsorption values found were always lower than

5-6 %. Therefore, it can be said that EtBr removal observed over such iron-doped titania catalysts took basically place by heterogeneous photocatalysis. On the other hand, it can be emphasized the relatively poor EtBr and TOC conversions achieved with the highest iron content catalyst (TiO_2-Fe5).

The relevancy of the EtBr adsorption step and its role on the degradation mechanism is pointed out upon a detailed UV spectroscopic monitoring of the EtBr bands during the course of the activity run. EtBr displays four transitions bands, one in the visible region at 480 nm, and three UV transitions at 343, 285, and 210 nm [13,25]. In Figure 3a it can be observed a monotonous decrease of EtBr bands upon increasing irradiation time for the TiO_2-Fe1 catalyst for which the EtBr adsorption step is considered almost negligible. In contrast, for TiO_2 sample (Figure 3b) a strong decrease of intensity of EtBr bands prior to turn on the UV lamp is exhibited as a consequence of EtBr adsorption. In comparison with the continuous decrease observed in TiO_2-Fe1 catalysts, in bare titania after 30 min. of irradiation, a gradual increase of a new wide band at about 265 nm can be observed. This emergent transition is in agreement with the formation of a photodesorbed intermediate inferred from TOC conversion evolution showed in Figure 2b for the TiO_2 catalyst, which is in accordance with similar results reported by other authors for degradation of amine type organic substances [26]. In conclusion, acid/basic surface character of the catalysts can modify not only the EtBr adsorption during the dark step but also the EtBr photodegradation mechanism.

Therefore, from the obtained results it can be considered that EtBr photodegradation over catalysts with iron content higher than 0.36 wt. % is not practically affected by chemisorption processes. Taking into account the overall obtained results the TiO_2-Fe1 specimen has been selected for further analysis since it provides highest TOC conversion level in the absence of significant EtBr adsorption phenomena.

3.3 Study of the efficiency of hydrogen peroxide for EtBr photodegradation.

To improve EtBr photodegradation performance a theoretical stoichiometric amount of H_2O_2 for complete oxidation of ethidium bromide to CO_2 and H_2O was

used during the EtBr photodegradation process with the selected TiO_2-Fe1 catalyst. EtBr and TOC conversions as a function of reaction times are shown in Figure 4, where the influence of the initial pH, 3.0 and 6.5, is also exhibited. EtBr photolysis run under these operating conditions reveals a gradual decrease of EtBr concentration (lower than 49% at 300 min. irradiation time) while no mineralization activity, i.e. complete oxidation to carbon dioxide and water reflected by TOC conversion, was detected.

Similar EtBr and TOC conversions were obtained with the TiO_2-Fe1 catalyst at the two studied pH, which makes difficult the selection of an optimal reaction pH. However, pH 3 was finally selected taking into account that hydrogen peroxide typically provides better efficiencies for degradation of other organic substances when working at acid pH [27].

To try to get total EtBr conversion with significant TOC removal, the influence of starting H_2O_2 concentration on EtBr photodegradation over TiO_2-Fe1 catalyst has been also studied in Figure 5 at initial pH = 3.0. In this case a theoretical (80 $mg \cdot L^{-1}$) and double of stoichiometric amount of H_2O_2 (160 $mg \cdot L^{-1}$) respectively for complete EtBr oxidation are displayed as a function of irradiation time at left side of Figure 5 (dosage 1).

Although higher EtBr and TOC conversion levels are always achieved with double of the H_2O_2 stoichiometric amount during the first 300 minutes, a lower H_2O_2 decomposition rate can be observed when employing the stoichiometric concentration.

Given that in any case the added H_2O_2 concentrations were sufficient to achieve total TOC removal, a new strategy to improve the final EtBr and TOC conversion levels was carried out. Thus, a second dosage of the corresponding starting hydrogen peroxide concentrations was added in both cases (dosage 2) when almost total hydrogen peroxide consumption had been attained after 300 min of reaction (see right side of Figure 5). Upon addition of such second dose, total EtBr conversions were achieved in both cases and a slight increase of TOC rate could be observed when the stoichiometric amount of H_2O_2 was used, reaching almost 80 % of TOC removal at 550 minutes. Ultimately, similar EtBr and TOC conversions are obtained even when the amount of oxidizing agent has been

doubled. Since it is known that H_2O_2-photoderived reactive hydroxyl radicals can attack the organic molecules but also can react between themselves or with other hydrogen peroxide molecules transforming into water and molecular oxygen [28], it must be taken into account that the presence of very high $^{\bullet}OH$ concentrations in the reaction medium could well provoke auto-scavenging reactions in detriment of organic matter oxidation [29,30]. In this sense, on the whole the results displayed in Fig. 5 are pointing out that using double of the stoichiometric H_2O_2 concentration in a second dosage favors hydroxyl radical scavenging effect, reducing the final photo-efficiency [29,30].

On this basis, it appears that control of the H_2O_2 dosing during reaction upon employing relatively low concentrations of H_2O_2 in multiple doses could minimize the mentioned scavenging effect. So, to achieve a better efficiency in the use of H_2O_2 during the photocatalytic process, small dosages of hydrogen peroxide were carried out during the EtBr photodegradation run. These results are shown in Figure 6, where the evolution of BrEt and TOC concentrations is given as a function of irradiation time.

The strategy used was to add small H_2O_2 concentrations during the photocatalytic process; the H_2O_2 concentration added at any given point was a function of the amount of TOC present at such point, introducing approximately the amount stoichiometrically required to completely oxidize the organic matter present in the reaction medium at that point (marked in Figure 6 as Dosage 1, 2, 3 and 4) until a final irradiation time of 9 hours. Total hydrogen peroxide concentrations of 196 $mg \cdot L^{-1}$ were added throughout the whole photocatalytic process in four dosages. This strategy of adding small H_2O_2 concentrations has led to around 84 % of organic matter removal at the end of the process, higher than TOC conversion level achieved with single dosing strategy (Figs. 4 or 5). Therefore, punctual dosages of H_2O_2 through irradiation time appear to minimize H_2O_2 self-scavenging reactions which leads to an apparent improvement of the final organic matter removal.

Finally, the selected iron doped titania catalyst (TiO_2-Fe1) has been reused in consecutive runs to determine its stability and durability during EtBr photocatalytic degradation. Hydrogen peroxide dosages in each cycle were

achieved following the same dosing strategy described in former paragraph, corresponding to a total amount of 196 $mg \cdot L^{-1}$ of H_2O_2 for every one of the 5 runs performed. These results are depicted in Figure 7, where it is represented the EtBr and TOC conversions and the iron leached detected at the end of each experiment. Total iron leached during the five consecutive runs corresponds to about 56 % of total Fe in the catalyst. The small amounts of iron detected at the end of some cycles could suggest that Photo-Fenton process could be also taking place during the photodegradation of EtBr. This fact has not been ruled out although the relatively low iron concentration detected joint to the fact that iron leaching is a slow and progressive process which is accompanied by short chain acids formation [31], leads us to suggest that the possible Photo-Fenton contribution must be very small or even negligible; this is particularly true for the last cycles where very residual iron amounts are detected. It must be noted in this sense that EtBr and TOC conversion levels achieved during the third run are similar or even higher than those achieved in the first cycle while the amount of leached iron is considerably lower in the former; in the fourth cycle, during which no leached iron was detected, TOC conversion suffers only a small decrease in comparison with the first cycle. Therefore, these results point out that heterogeneous photocatalysis rather than homogeneous Photo-Fenton play most relevant role in any case.

In spite of the detected iron losses, relatively good photodegradation efficiency was attained in all the runs although it can be observed a decrease in final TOC removal after the fourth cycle. This fact is pointing out to the existence of some catalysts deactivation phenomena, which was more pronounced in the fifth cycle, in which no total hydrogen peroxide consumption was observed with only 46 % of TOC conversion being obtained.

To clarify the deactivation phenomena observed in the TiO_2-Fe1 catalysts the analysis of some of the used catalysts by XPS was carried out. Four used TiO_2-Fe1 catalysts were recovered after four of the performed runs and compared with the fresh TiO_2-Fe1 catalyst. Thus, the TiO_2-Fe1 catalyst used with 160 $mg \cdot L^{-1}$ and 320 $mg \cdot L^{-1}$ of H_2O_2 (Figure 5), TiO_2-Fe1 used in the control H_2O_2 dosage reaction

(Figure 6), and the TiO_2-Fe1 catalyst used in the consecutives runs (Figure 7) were recovered and Fe, Ti, O, C and N regions were analyzed by XPS.

The XPS spectra at the N1s binding energy zone of these TiO_2-Fe1 catalysts after reactions with different hydrogen peroxide concentrations at pH 3 are shown in Figure 8. It must be noted that the existence of N1s core level contributions are only observed in the used catalysts which means that nitrogen atoms derived from EtBr molecule or its decomposition as amine type by-products become adsorbed over the catalyst surface during the photo-degradation process. The fitting of N1s spectra shows the presence of four components at about the following binding energies: 397.1 eV, 398.7 eV, 399.9 eV and 401.5 eV. According to the literature [32], the peak at 397.1 eV can correspond to M-N linkages that could correspond to formation of surface Ti-N or Fe-N complexes during the adsorption process and/or favored by the UV light [32,33]. The N1s component at ca. 398.7 eV has been assigned to contributions from N bonded to C through simple or double bonds, N-C and –C=NH bonds [34,35], in species as $PhNH_2$ [36] and in pyridine-type structures [37]. The components at higher binding energies (399.9 eV and 401.5 eV) are closer to those for NH_x moieties in organic species as amine groups [37], adsorbed NH_3 [38] and/or charged nitrogen or ammonia groups [39,40].

Finally, on Table 2 are summarized the final TOC removal achieved during each corresponding EtBr photodegradation run, the iron content in fresh and used catalysts respectively, joint to $(Fe/Ti)_{XPS}$ atomic ratios and N % measured by XPS. Most of the differences found in the used catalysts analysis compared with the fresh catalyst are related to the surface nitrogen percentage and iron losses from these catalysts during the EtBr degradation. It can be observed that important iron losses have been detected in all used catalysts, especially in the case of the catalyst used in consecutive runs. At the same time, significant increases in iron surface content can be observed from used catalysts in comparison with the fresh one, despite the global loss of iron from the catalyst as a consequence of leaching. In this respect, it is well known that iron lixiviation can take place by carboxylic acid extraction [41,42], while iron lixiviation/re-adsorption phenomena on this type of iron-doped titania catalyst was observed in the solar

photocatalytic degradation of phenol [31]; therefore, a similar mechanism could be taking place in this case given the higher surface iron content detected over the used catalysts. This mechanism is not as evident in the catalyst used during five cycles. In this case, the $(Fe/Ti)_{XPS}$ atomic ratio decreases, which must be due to the high loss of iron produced on the whole during such long test.

On the other hand, it may be noted that when final TOC conversions achieved at the end of the experiment are higher, surface nitrogen percentage detected in the used catalysts decreases. Such results suggest that catalyst deactivation, by surface poisoning due to amine type by-product formation, takes place to a degree which depends mainly on the length of the test but also on other experimental conditions (Table 2); we cannot discard however some contribution to deactivation from formation in some case of certain refractory intermediates (as amine type), which usually are difficult to degrade [43]. On the other hand, a more simple explanation for catalyst deactivation could be related to the observed iron loss, principally from the surface of the catalyst, considering results obtained as a function of iron content (Fig. 2).

4. Conclusions

A series of nanosized iron-doped titania catalysts have been studied for the photocatalytic degradation of Ethidium Bromide (EtBr) with oxygen. EtBr photocatalytic degradation and its mechanism are dominated by an initial EtBr adsorption step whose strength depends on acid/base surface properties of the catalysts. Such chemisorption phenomenon is shown to be favored for slightly basic surfaces present in undoped TiO_2 or a catalyst with relatively low iron doping level (0.36 wt. %) and apparently favor generation of more refractory organic intermediates photodesorbed in the reaction medium. On the basis of such results, a catalyst with intermediate iron content (TiO_2-Fe1) was selected as optimum one since it displays highest TOC conversion levels in the absence of significant EtBr adsorption phenomena.

On the other hand, the efficiency in the use of H_2O_2 as oxidant has been also explored in order to define the best operating conditions. A better efficiency of the consumption of H_2O_2 in EtBr photodegradation was obtained when using the

stoichiometric amount of H_2O_2 in two consecutive dosages getting an important improvement in organic matter removal. This study has allowed to establish a new strategy to improve final EtBr and TOC conversions, which is related to the control of hydrogen peroxide dosing along irradiation time in order to minimize hydroxyl radicals self-scavenging reactions.

Finally, the selected iron doped titania catalyst (TiO_2-Fe1) has been reused in consecutive runs in order to determinate its stability and durability. A catalyst deactivation phenomenon is detected after 5 consecutive runs of 9 hours each due to iron losses and/or generation of surface N-containing poison molecules; nevertheless, very good photodegradation efficiency could be achieved in any case, with around 80 % of TOC removal being attained after 40 consecutive hours.

Acknowledgements

Authors would like to thank Prof. J.L.G. Fierro for the performance and unconditional help in the interpretation of XPS spectra of the used catalysts. We gratefully acknowledge the Spanish MICINN for the financial support of the CTM2007-60577/TECNO project, and J. Carbajo also acknowledges the FPI grant to the MICINN.

References

[1] L. Bountiff, P. Levantis, J. Oxford, Electrophoretic analysis of nucleic acids isolated from scrapie-infected hamster brain, J. Gen. Virology 77 (1996) 2371-2378.

[2] J. Duhamel, J. Kanyo, G. Dinter-Gottlieb, P. Lu, Fluorescence emission of EB intercalated in defined DNA duplexes: hydrodynamics and base pair twisting components, Biochemistry 35 (1996) 16687-16697.

[3] J.T. MacGregor, I.J. Johnson, In vitro metabolic activation of ethidium bromide and other phenanthridinium compounds: Mutagenic activity in *Salmonella typhimurium*, Mutation Res. 48 (1977) 103–108.

[4] H. Joshua, Quantitative adsorption of ethidium bromide from aqueous solutions by macroreticular resins, Biotechniques 4 (3) (1986) 207-208.

[5] M. Yamada, K. Kato, M. Nomizu, N. Sakairi, K. Ohkawa, H. Yamamoto, N. Nishi, Preparation and characterization of DNA films induced by UV irradiation, Chem. Eur. J., 8 (6) (2002) 1407-1412.

[6] C.S. Zhao, S.D. Sun, K.G. Yang, M. Nomizu, N. Nishi, DNA-loaded porous polyethersulfone particles for environmental applications I. preparation, J. Appl. Polym. Sci., 98 (4) (2005) 1668-1673.

[7] C.S. Zhao, K.G. Yang, X. Wen, F. Li, B.X. Zheng, M. Nomizu, N. Nishi, DNA-loaded porous polyethersulfone particles for environmental applications II. Utilization, J. Appl. Polym. Sci., 98 (4) (2005) 1674-1678.

[8] R. Zocher, A. Billich, U. Keller, P. Messner, Destruction of Ethidium Bromide in Solution by Ozonolysis, Biol. Chem. Hoppe Seyler, 369 (10) (1988) 1191-1194

[9] Massachusetts Institute of Technology (MIT). http://web.mit.edu/environment/pdf/SYBR.pdf (March 2006).

[10] S. Malato, J. Blanco, A. Vidal, C. Richter. Photocatalysis with solar energy at pilot-plant scale: an overview. Appl. Catal. B: Environ. 37 (2002) 1-15.

[11] J. Blanco, S. Malato, P. Fernández, A. Vidal, A. Morales, P. Trincado, J.C. Oliveira, C. Minero, M. Musci, C. Casalle, M. Brunotte, S. Tratzky, N. Dischinger, K.H. Funken, C. Sattler, M. Vincent, M. Collares-Pereira, J.F. Mendez y C.M. Rangel, Compound parabolic concentrator technology development to

commercial solar detoxification applications, Sol. Energy, 67 (4-6) (2000) 317-330.

[12] M. Faisal, M. Abu Tariq, M. Muneer, Photocatalysed degradation of two selected dyes in UV-irradiated aqueous suspensions of titania, Dyes and Pigments 72 (2007) 233-239.

[13] C. Adán, A. Bahamonde, A. Martínez-Arias, M. Fernández-García, L. A. Pérez-Estrada, S. Malato, Solar light assisted photodegradation of ethidium bromide over titania-based catalysts, Catal. Today 129 (2007) 79-85.

[14] C. Adán, A. Martínez-Arias, M. Fernández-García, A. Bahamonde, Photocatalytic degradation of ethidium bromide over titania in aqueous solutions, Appl. Catal. B: Environ. 76 (2007) 395-402.

[15] J. R. Rodríguez, J. Beltrán, O. Rodríguez, Vis and UV photocatalytic detoxification methods (using TiO_2, TiO_2/H_2O_2, TiO_2/O_3, $TiO_2/S_2O_8^{2-}$, O_3, H_2O_2, $S_2O_8^{2-}$, Fe^{2+}/H_2O_2 and $Fe^{3+}/H_2O_2/C_2O_4^{2-}$) for dyes treatment, Catal. Today 101, (2005) 389-395.

[16] A. Fuerte, M. D. Hernández-Alonso, A. J. Maira, A. Martínez-Arias, M. Fernández-García, J. C. Conesa, J. Soria, G. Munuera, Nanosize Ti–W mixed oxides: effect of doping level in the photocatalytic degradation of toluene using sunlight-type excitation, J. Catal. 212 (1) (2002) 1-9.

[17] S. Eriksson, U. Nylén, S. Rojas, M. Boutonnet, Preparation of catalysts from microemulsions and their applications in heterogeneous catalysis, Appl. Catal. A: Gen. 265 (2004) 207-219.

[18] C. Adán, A. Bahamonde, M. Fernández-García, A. Martínez-Arias, Structure and activity of nanosized iron-doped anatase TiO_2 catalysts for phenol photocatalytic degradation, Appl. Catal. B: Environ. 72 (2007) 11-17.

[19] R. Jenkins, R. L. Zinder, Introduction to X-Ray power Diffractometry, John Wisley & Sons Inc, New York, 1996.

[20] C.D. Wagner, L.E. Davis, M.V. Zeller, J.A. Taylor, R.H. Raymond, L.H. Gale, Empirical atomic sensitivity factors for quantitative analysis by electron spectroscopy for chemical analysis, Surf. Interface Anal. 3 (5) (1981) 211-225.

[21] B. Hundson, R. Jacobs. The ultraviolet transitions of the ethidium cation, Biopolymers, 14 (6) (1995)1309-1312.

[22] G.M. Eisenberg, Colorimetric determination of hydrogen peroxide, Ind. Eng. Chem. Anal. 15 (5) (1943) 327-328.

[23] J. Araña, O. González Díaz, J.M. Rodríguez, J.A. Herrera Melián, C. Garriga i Cabo, J. Pérez Peña, M. Carmen Hidalgo, J.A. Navío-Santos, Role of Fe^{3+} /Fe^{2+} as TiO_2 dopant ions in photocatalytic degradation of carboxylic acids, J. Mol. Catal. A Chem. 197 (2003) 157-171.

[24] A. Di Paola, E. García-López, G. Marcì, C. Martín, L. Palmisano, V. Rives, A. M. Venecia, Surface characterization of metal ions loaded TiO_2 photocatalysts: structure-activity relationship, Appl. Catal. B 48 (2004) 223-233.

[25] B. Hundson, R. Jacobs, The Ultraviolet Transitions of the Ethidium Cation. Biopolymers 14 (1975) 1309-1312.

[26] B.F. Abramovic, V.B. Anderluh, A.S. Topalov, F.F. Gaál, Titanium dioxide mediated photocatalytic degradation of 3-amino-2-chloropyridine, Appl. Catal. B Environ., 48 (2004) 213-221.

[27] S. Malato, P. Fernández-Ibáñez, M. I. Maldonado, J. Blanco, W. Gernjak. Decontamination and desinfection of water by solar photocatalysis: recent overview and trends. Catal. Today 147 (2009) 1-59.

[28] W. P. Kwan, B. M. Voelker. Influence of electrostatics on the oxidation rates of organic compounds in heterogeneous Fenton systems. Environ. Sci. Technol. 38 (12) (2004) 3425-3431.

[29] B. Tryba, A.W. Morawski, M. Inagaki, M. Toyoda, The kinetics of phenol decomposition under UV irradiation with and without H_2O_2 on TiO_2 ,Fe–TiO_2 and Fe–C–TiO_2 photocatalysts, Appl. Catal. B: Environ. 63 (2006) 215-221.

[30] C. Adán, J. Carbajo, A. Bahamonde, A. Martínez-Arias, Phenol photodegradation with oxygen and hydrogen peroxide over TiO_2 and Fe-doped TiO_2, Catal. Today 143 (3-4) (2009) 247-252.

[31] C. Adán, A. Martinez-Arias, S. Malato, A. Bahamonde. New insights on solar photocatalytic degradation of phenol over fe-TiO2 catalysts: Photo-complex mechanism of iron lixiviates. Appl. Catal. B: Environ. 93 (2009) 96-105.

[32] X-Z. Shen, Z-C. Liu, S-M. Xie, J. Guo, Degradation of nitrobenzene using titania photocatalyst co-doped with nitrogen and cerium under visible light illumination, J. Hazard. Mater. 162 (2009) 1193-1198.

[33] R.D. Willebruch, C.R. Clayton, M. Oversluizen, D. Kim, Y. Lu, An XPS and electrochemical study of the influence of molybdenum and nitrogen on the passivity of austenitic stainless steel, Corrosion Sci., 31 (1990) 179-190.

[34] F. Le Normand, J. Hommet, T. Szorenyi, C. Fuchs, E. Fogarassy, XPS study of pulsed laser deposited CN_x films, Phys. Rev. B 64 (23) (2001) 235416-235431.

[35] C. Ronning, H. Feldermann, R. Merk, H.Hofsass, P. Reinke, J. U. Thiele, Carbon nitride deposited using energetic species: a review on XPS studies, Phys. Rev. B 58 (4) (1998) 2207-2215.

[36] C. Jones, E. Sammann, The effect of low power plasmas on carbon fibre surfaces, Carbon 28 (4) (1990) 509-514.

[37] T. Nakajima, M. Koh, Synthesis of high crystalline carbon-nitrogen layered compounds by CVD using nickel and cobalt catalysts, Carbon 35 (2) (1997) 203-208.

[38] P. Marcus, M.E. Bussel, XPS study of the passive films formed on nitrogen-implanted austenitic stainless steels, Appl. Surf. Sci. 59 (1992) 7-21.

[39] R. Pietrzak, XPS study and physico-chemical properties of nitrogen-enriched microporous activated carbon from high volatile bituminous coal**,** Fuel 88 (2009) 1871-1877.

[40] G. Tzvetkov, G. Koller, Y. Zubavichus, O. Fuchs, M.B. Casu, C. Heske, E. Umbach, M. Grunze, M.G. Ramsey, F.P. Netzer, Bonding and structure of glycine on ordered Al_2O_3 film surfaces, Langmuir 20 (2004) 10551-10559.

[41] J. Zazo, J. A. Casas, A. F. Mohedano, J. J. Rodríguez. Catalytic wet peroxide oxidation of phenol with a Fe/active carbon catalyst. Appl. Catal. B. Environ. 65 (2006) 261-268

[42] F. J. Beltrán, F. J. Rivas, R. Montero-de-Espinosa. Iron type catalyst for the ozonation of oxalic acid water. Water Res. 39 (2005) 3553-3564

[43] L. Akiengesellschaft (Inv. K. Dietmar), USP 5043075, Method of removing amines, (Aug. 27, 1991).

Figure 1

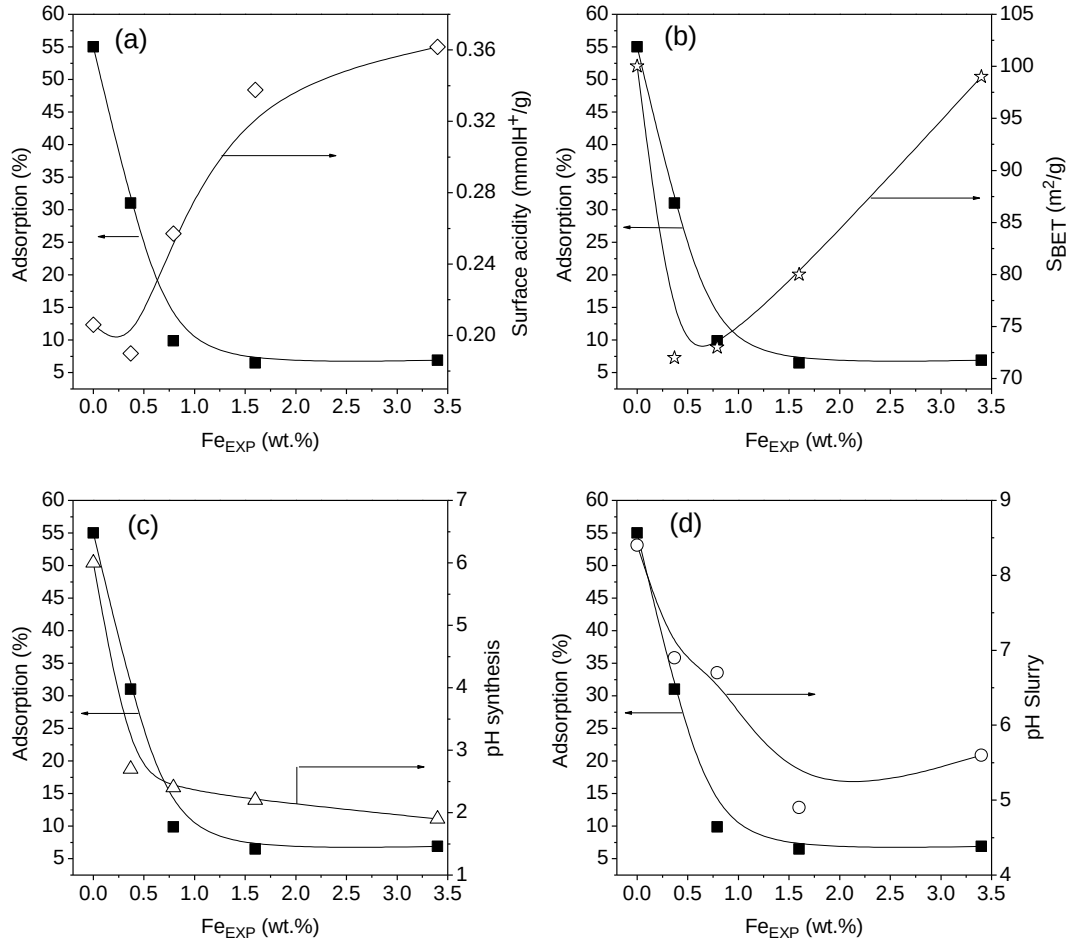
(a)
Adsorption (%)
Surface acidity (mmolH+/g)
FeEXP (wt.%)
(b)
Adsorption (%)
SBET (m2/g)
FeEXP (wt.%)
(c)
Adsorption (%)
pH synthesis
FeEXP (wt.%)
(d)
Adsorption (%)
pH Slurry
FeEXP (wt.%)

Figure 2

.

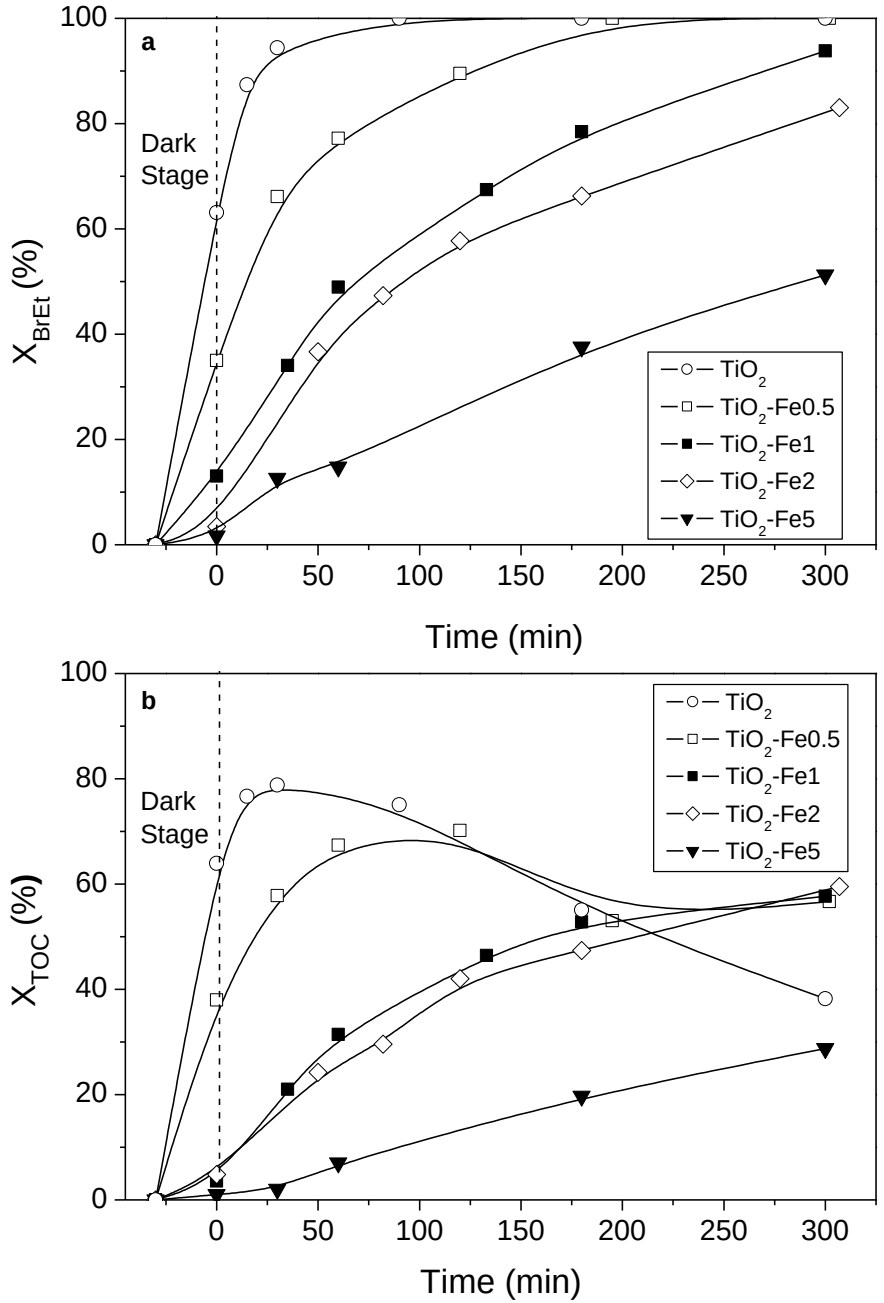
a
Dark
Stage
X_{BrEt} (%)
Time (min)
TiO2
TiO2-Fe0.5
TiO2-Fe1
TiO2-Fe2
TiO2-Fe5
b
Dark
Stage
X_{TOC} (%)
Time (min)
TiO2
TiO2-Fe0.5
TiO2-Fe1
TiO2-Fe2
TiO2-Fe5

Figure 3

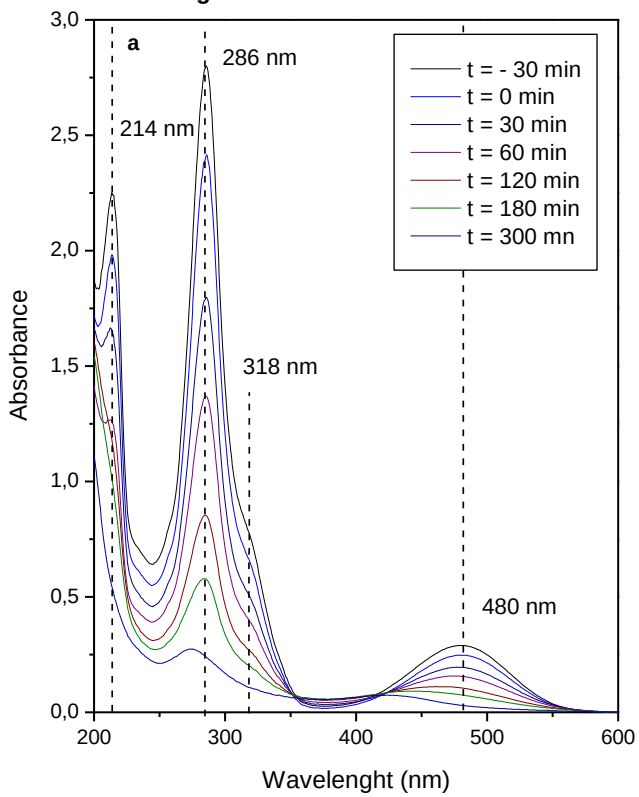
a
286 nm
214 nm
318 nm
480 nm
t = - 30 min
t = 0 min
t = 30 min
t = 60 min
t = 120 min
t = 180 min
t = 300 mn
Absorbance
Wavelenght (nm)

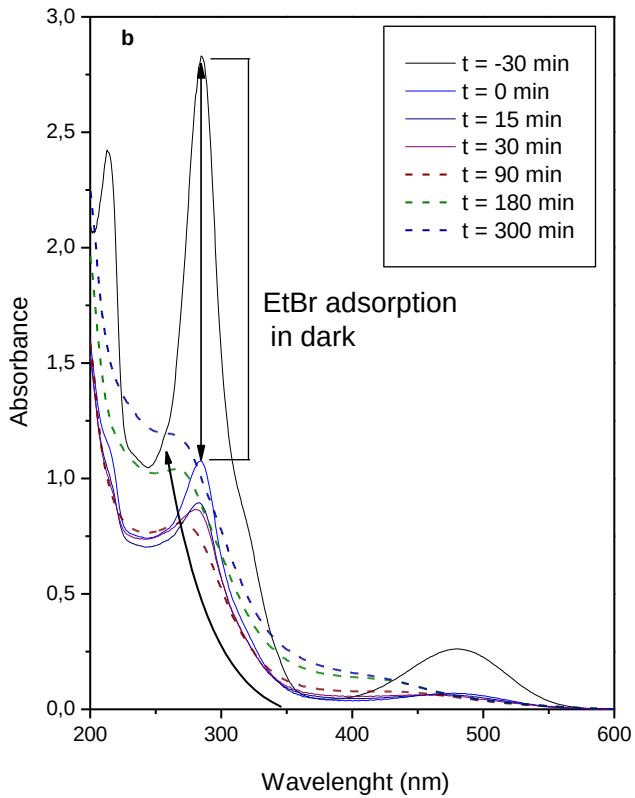
b
t = -30 min
t = 0 min
t = 15 min
t = 30 min
t = 90 min
t = 180 min
t = 300 min
EtBr adsorption
in dark
Absorbance
Wavelenght (nm)

Figure 4

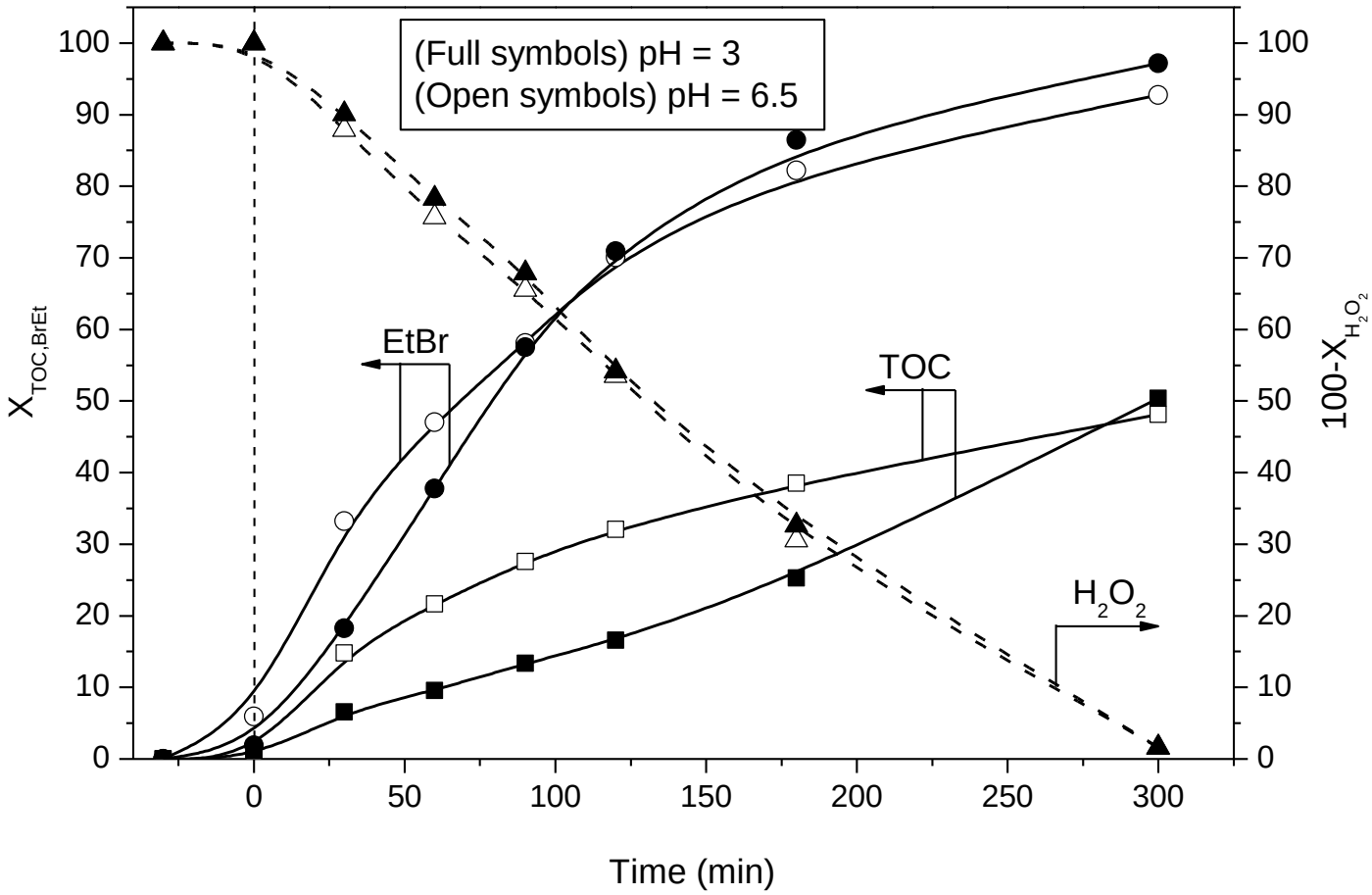
(Full symbols) pH = 3
(Open symbols) pH = 6.5
EtBr
TOC
H2O2
X TOC,BrEt
100-X H2O2
Time (min)
0
10
20
30
40
50
60
70
80
90
100
0
50
100
150
200
250
300

Figure 5

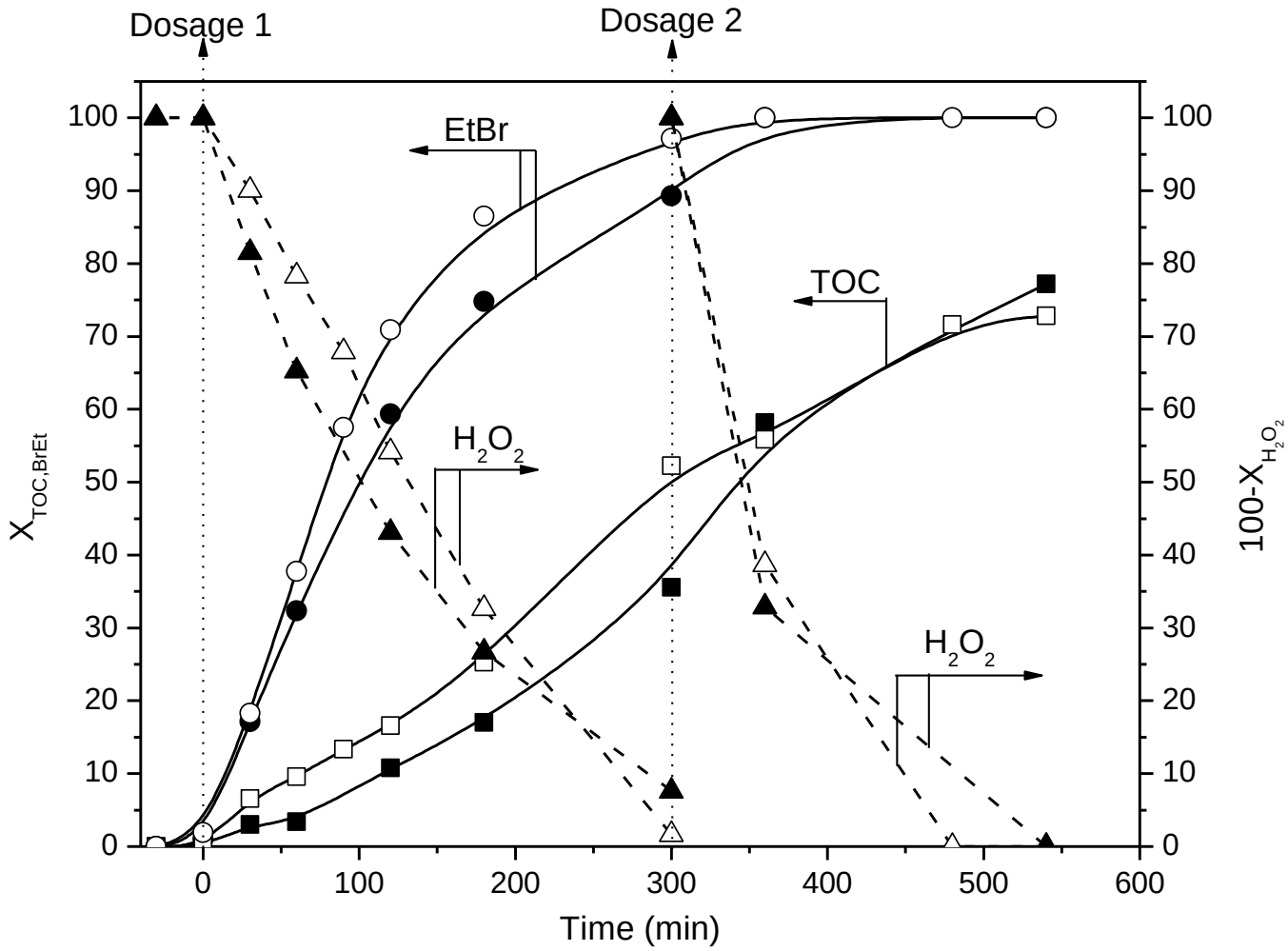
Dosage 1
Dosage 2
EtBr
TOC
H2O2
H2O2
X TOC,BrEt
100-X H2O2
Time (min)
0
100
200
300
400
500
600
0
10
20
30
40
50
60
70
80
90
100

Figure 6

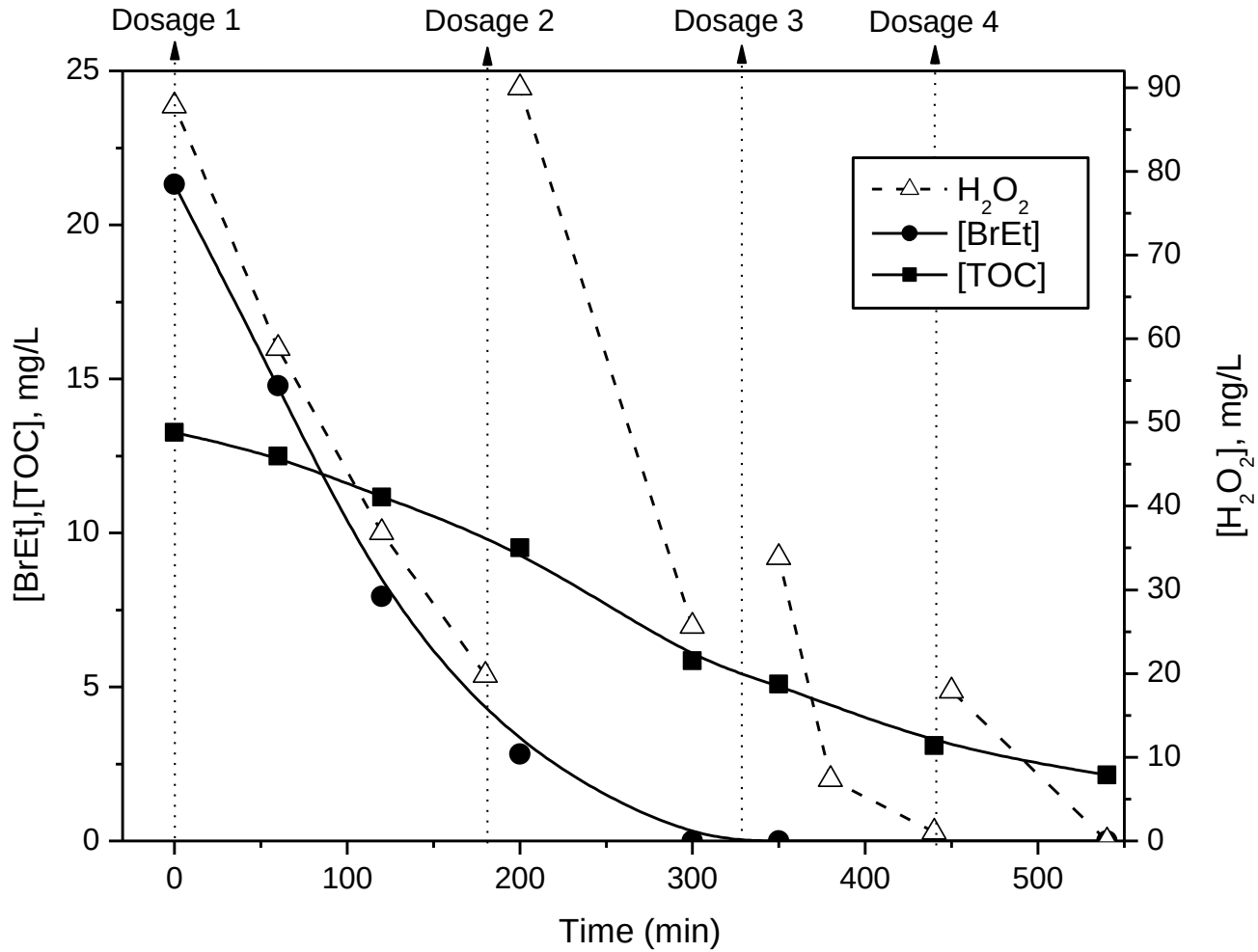
Dosage 1
Dosage 2
Dosage 3
Dosage 4
H2O2
[BrEt]
[TOC]
[BrEt],[TOC], mg/L
[H2O2], mg/L
Time (min)
0
5
10
15
20
25
0
10
20
30
40
50
60
70
80
90
0
100
200
300
400
500

Figure 7

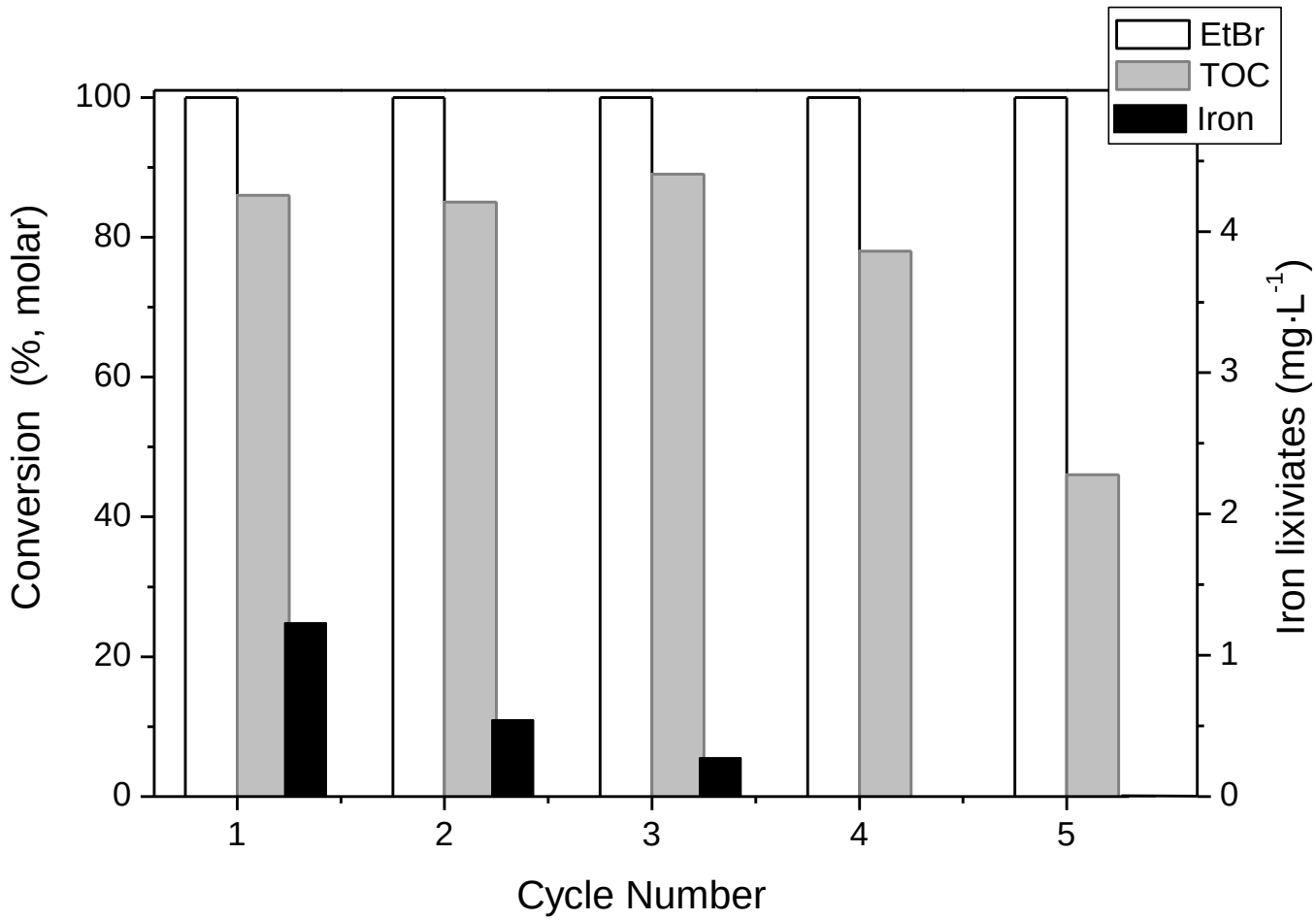
EtBr
TOC
Iron
Conversion (%, molar)
Iron lixiviates (mg·L-1)
Cycle Number
0
20
40
60
80
100
0
1
2
3
4
1
2
3
4
5

Figure 8

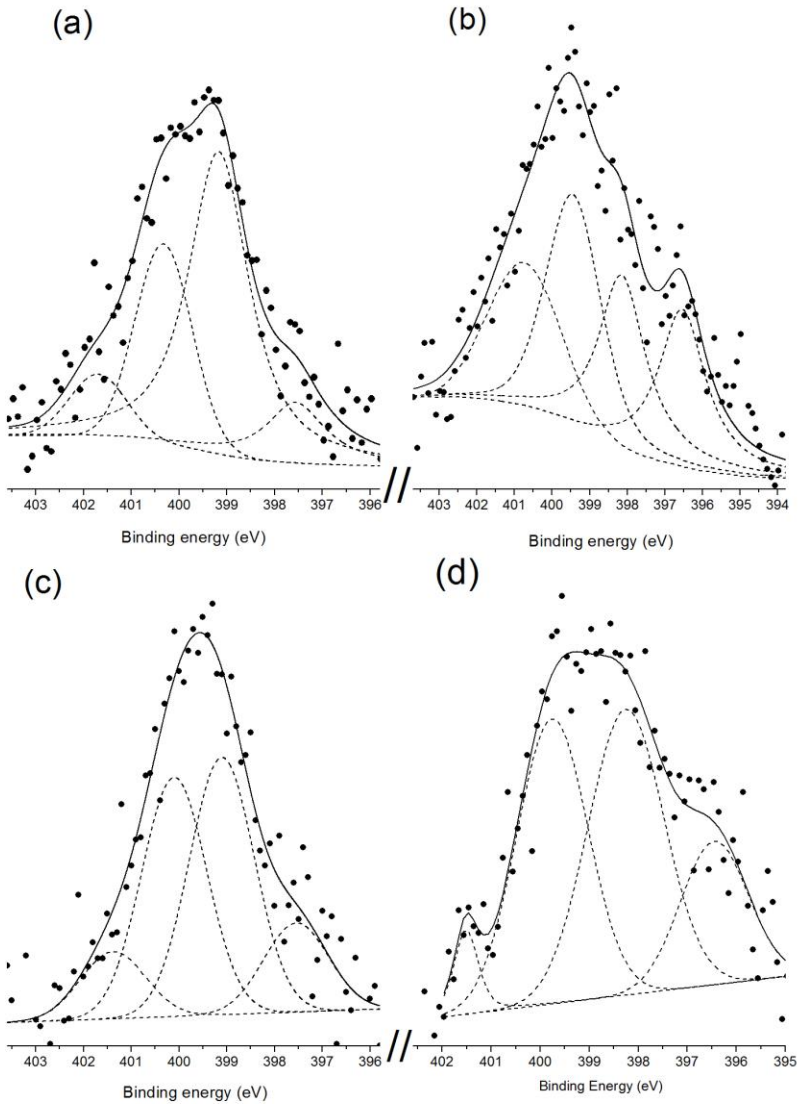
(a)
403 402 401 400 399 398 397 396
Binding energy (eV)
(b)
403 402 401 400 399 398 397 396 395 394
Binding energy (eV)
(c)
403 402 401 400 399 398 397 396
Binding energy (eV)
(d)
402 401 400 399 398 397 396 395
Binding Energy (eV)

Table 1. - Physico-chemical properties of TiO_2-Fe catalysts.

Catalysts	**$Fe_{Catalyst}$ (wt %)**	**d_A[a] (nm)**	**S_{BET} (m^2/g)**
TiO_2	0.00	8.6	100
TiO_2-Fe0.5	0.36	9.8	72
TiO_2-Fe1	0.72	11.0	73
TiO_2-Fe2	1.60	11.0	80
TiO_2-Fe5	3.40	9.4	99

[a] Crystal size of the anatase phase from diffraction peak at $2\theta \approx 25.28^{o}$, using the Scherrer equation.

Table 2. Iron content, atomic ratios and total surface nitrogen percentage on used TiO_2-Fe1 catalyst.

EtBr photodegradation run	**X_{TOC} (%)[a]**	**$Fe_{catalyst}$ (wt. %)**	**Fe_{Lix} ($mg \cdot L^{-1}$)**	**Fe_{Lix} (%)**	**$(Fe/Ti)_{XPS}$**	**% N_{XPS}[c]**
Reference: fresh catalyst	-	0.72	-	-	0.010	0.00
$[H_2O_2]_o$=160 $mg \cdot L^{-1}$ (Fig. 5)	77	0.43	0.67	18.6	0.014	1.73
$[H_2O_2]_o$=320 $mg \cdot L^{-1}$ (Fig. 5)	72	0.41	0.88	24.4	0.034	2.20
Control H_2O_2 dosage (Fig. 6)	84	0.40	0.76	21.1	0.024	1.14
Consecutive runs (Fig. 7)	46[b]	0.27	2.02	56.1	0.007	1.57

[a] Irradiation time = 540 min

[b] TOC conversion in the last consecutive cycle

[c] Ratio of total surface nitrogen: $\%N_{XPS} = \frac{N/Ti}{N/Ti + Fe/Ti + C/Ti + O/Ti + Ti/Ti} \times 100$